Unification of the Kirchhoff approximation and the method of moment for optical wave scattering from the lossy dielectric Gaussian random rough surface

Jun Ma (麻 军)*, Lixin Guo (郭立新), and Xiangzhe Cheng (程相哲)

School of Science, Xidian University, Xi'an 710071

**E-mail: clack2006@163.com*

Received July 3, 2008

The optical wave scattering from one-dimensional (1D) lossy dielectric Gaussian random rough surface is studied. The tapered incident wave is introduced into the classical Kirchhoff approximation (KA), and the shadowing effect is also taken into account to make the KA results have a high accuracy. The definition of the bistatic scattering coefficient of the modified KA and the method of moment (MOM) are unified. The characteristics of the optical wave scattering from the lossy dielectric Gaussian random rough surface of different parameters are analyzed by implementing MOM.

OCIS codes: 290.5880, 290.0290, 240.0240.

doi: 10.3788/COL20090703.0259.

The study on optical wave scattering from random rough surface has been the subject of intensive investigation over the past several decades for the application in a number of important research areas such as characterization of films and optical interface, and the design of optical scanning instrument for use in the semiconductor industry[1−6]. The characteristic of optical wave scattering by one-dimensional (1D) conducting rough surface is studied by the angular correlation functions of the polarized scattered intensities[7]. Among the many rough surface theories for calculating scattering, the Kirchhoff approximation (KA)[8] and the method of moment (MOM)[9] are widely used. KA is an analytical method and MOM is a numerical method. In this letter, the characteristic of optical wave scattering from the lossy dielectric Gaussian random rough surface is studied by the bistatic scattering coefficient. The tapered incidence, which is commonly used in the MOM for calculating rough surface scattering, is introduced into the classical KA. The emphasis is put on studying the unification of the definition of the bistatic scattering coefficient by KA and MOM. The numerical results of the optical wave scattering from the lossy dielectric rough surface are also compared with these methods, and the influence of the shadowing effect is taken into account in KA so as to make the results have a high accuracy.

Considering an incident wave $\varphi^{\rm inc}(\vec{r})$ impinging upon a random rough surface with the height profile $z = f(x)$, as shown in Fig. 1. ε_0 and ε_1 are the relative dielectric constants of the free space and the lower medium space, and $\varepsilon_0 = 1$. $f(x)$ is a Gaussian distributed rough surface with the correlation length l and the root mean square (RMS) height h. The spectral density of 1D Gaussian random rough surface is[8]

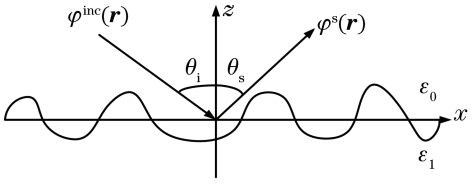

Fig. 1. Geometry of optical wave scattering from the Gaussian rough surface.

$$W(k) = \frac{h^2 l}{2\sqrt{\pi}} \exp(-\frac{-k^2 l^2}{4}). \tag{1}$$

In this letter, the optical wave scattering by 1D lossy dielectric Gaussian rough surface is studied by the total electric field for the horizontal polarization and the total magnetic field for the vertical polarization, respectively. For the horizontal polarization, the total electric field of the optical wave is $\vec{E}(\vec{r}) = \varphi(\vec{r})\hat{y}$, and for the vertical polarization, the total magnetic field of the optical wave is $\vec{H}(\vec{r}) = \varphi(\vec{r})\hat{y}$. The time dependence is $\mathrm{e}^{-\mathrm{i}\omega t}$.

From the spectral density, the Gaussian rough surface $f(x)$ can be simulated by Monte Carlo method[9]. In the two-dimensional (2D) scattering problem $\vec{r} = x\hat{x} + z\hat{z}$, the total wave function $\varphi(\vec{r})$ is

$$\varphi(\vec{r}) = \varphi^{\rm inc}(\vec{r}) + \varphi^{\rm s}(\vec{r}), \tag{2}$$

where $\varphi^{\rm s}(\vec{r})$ is the scattered wave, which can be written as[10]

$$\begin{aligned}\varphi^{\rm s}(\vec{r}) &= \varphi(\vec{r}) - \varphi^{\rm inc}(\vec{r}) \\ &= \int_s \left[\varphi(\vec{r}\,')\frac{\partial G(\vec{r},\vec{r}\,')}{\partial n'} - G(\vec{r},\vec{r}\,')\frac{\partial \varphi(\vec{r}\,')}{\partial n'}\right] \mathrm{d}s',\end{aligned} \tag{3}$$

$G(\vec{r},\vec{r}\,')$ is the 2D Green's function and $G(\vec{r},\vec{r}\,') = \frac{\mathrm{i}}{4}H_0^{(1)}(k_0\,|\vec{r}-\vec{r}\,'|)$, where k_0 is the wave number of the free space and $H_0^{(1)}(\cdot)$ is the zeroth order Hankel function of the first kind. The normal derivative of the Green's function is given by[11]

$$\frac{\partial G(\vec{r},\vec{r}\,')}{\partial n'} = \frac{\mathrm{i}k_0}{4}\hat{n}' \cdot \frac{\vec{r}-\vec{r}\,'}{|\vec{r}-\vec{r}\,'|} H_1^{(1)}(k_0\,|\vec{r}-\vec{r}\,'|), \tag{4}$$

$\hat{n}'$ is the unit normal vector of the rough surface, $\hat{n}' = \frac{-f'(x')\hat{x}+\hat{z}}{\sqrt{1+[f'(x')]^2}}$, $f'(x')$ is the first order derivative of $f(x')$, and $H_1^{(1)}(\cdot)$ is the first order Hankel function of the first kind. Here, the Kirchhoff approximation is applied to solve Eq. (3). If the Fresnel reflection coefficient for the incident wave onto a plane surface is denoted by R, then the total wave on the surface is given by[10]

$$\varphi(\vec{r}') = (1+R)\varphi^{\mathrm{inc}}(\vec{r}'). \tag{5}$$

And R satisfies

$$R_{\mathrm{HH}}(\theta_{\mathrm{i}}) = \frac{\varepsilon_1 \cos\theta_{\mathrm{i}} - (\varepsilon_1 - \sin^2\theta_{\mathrm{i}})^{1/2}}{\varepsilon_1 \cos\theta_{\mathrm{i}} + (\varepsilon_1 - \sin^2\theta_{\mathrm{i}})^{1/2}}, \tag{6a}$$

$$R_{\mathrm{VV}}(\theta_{\mathrm{i}}) = \frac{\cos\theta_{\mathrm{i}} - (\varepsilon_1 - \sin^2\theta_{\mathrm{i}})^{1/2}}{\cos\theta_{\mathrm{i}} + (\varepsilon_1 - \sin^2\theta_{\mathrm{i}})^{1/2}} \tag{6b}$$

for HH polarization and VV polarization, respectively, with θ_{i} representing the incidnt angle. To avoid artificial edge diffraction, the incident wave cannot be expressed as a plane wave, but as a tapered wave in which the energy is distributed in a narrow beam about the mean incident angle. The tapered plane wave developed by Thorsos[8] satisfies this requirement and is chosen as the incident wave. Considering a tapered plane wave incident on the rough surface, the incident wave can be expressed as[8]

$$\varphi^{\mathrm{inc}}(\vec{r}') = \exp\{\mathrm{i}k_0[x'\sin\theta_{\mathrm{i}} - f(x')\cos\theta_{\mathrm{i}}][1+w(\vec{r}')]\} \times \exp\left\{-\frac{[x'+f(x')\tan\theta_{\mathrm{i}}]^2}{g^2}\right\}, \tag{7}$$

where $w(\vec{r}') = [2(x'+f(x')\tan\theta_{\mathrm{i}})^2/g^2 - 1]/(k_0 g\cos\theta_{\mathrm{i}})^2$, g is the tapering parameter with the dimension and controls the tapering of the incident wave. As the basis of the tapered incident wave, the tapering parameter g and L should at least satisfy all requirements of the wave equation, correlation length, and energy truncation, which results in[12]

$$g > \frac{6}{(\cos\theta_{\mathrm{i}})^{1.5}}, \tag{8}$$

$$L > 15l \qquad \text{and} \qquad L \geq 4g. \tag{9}$$

Here, we choose $g = L/4$. From Eq. (4), the normal derivative of the total wave function can be written as[10]

$$\frac{\partial\varphi(\vec{r}')}{\partial n'} = (1-R)\frac{\partial\varphi^{\mathrm{inc}}(\vec{r}')}{\partial n'}, \tag{10}$$

where $\frac{\partial\varphi^{\mathrm{inc}}(\vec{r}')}{\partial n'} = (\nabla'\varphi^{\mathrm{inc}}(\vec{r}')\cdot\hat{n}')$, which can be written as

$$\frac{\partial\varphi^{\mathrm{inc}}(\vec{r}')}{\partial n'} = \varphi^{\mathrm{inc}}(\vec{r}') \times \left[-f'(x')P_1 + \frac{2(x'+f(x')\tan\theta_{\mathrm{i}})}{g^2}P_2 + P_3 + \frac{2\tan\theta_{\mathrm{i}}(x'+f(x')\tan\theta_{\mathrm{i}})}{g^2}P_2\right], \tag{11}$$

where $P_1 = \mathrm{i}k_0\sin\theta_{\mathrm{i}}(1+w(\vec{r}'))$, $P_2 = \mathrm{i}k_0(x'\sin\theta_{\mathrm{i}} - f(x')\cos\theta_{\mathrm{i}})\frac{2}{(k_0 g\cos\theta_{\mathrm{i}})^2} - 1$, $P_3 = -\mathrm{i}k_0(1+w(\vec{r}'))$. With far-field restriction, the following relationship then holds for the argument of the Green's function $k_0|\vec{r}-\vec{r}'| \approx k_0 r - k\hat{r}\cdot\vec{r}'$, where $\hat{r}$ is the unit vector in the $\vec{r}$ direction. The normal derivative of the Green's function is similarly evaluated, making the additional assumption that $k_0|\vec{r}-\vec{r}'| \gg 1$, which is equivalent to $kr \gg 1$. The Green's function and its normal derivative become as follows

$$G(\vec{r},\vec{r}') \approx \sqrt{\frac{\mathrm{i}}{8\pi k_0 r}}\exp(\mathrm{i}k_0 r)\exp(-\mathrm{i}\vec{k}_{\mathrm{s}}\cdot\vec{r}'), \tag{12a}$$

$$\frac{\partial G(\vec{r},\vec{r}')}{\partial n'} \approx \sqrt{\frac{\mathrm{i}}{8\pi k_0 r}}\exp(\mathrm{i}k_0 r)\exp(-\mathrm{i}\vec{k}_{\mathrm{s}}\cdot\vec{r}')(-\mathrm{i}\vec{k}_{\mathrm{s}}\cdot\hat{n}'), \tag{12b}$$

where $\vec{k}_{\mathrm{s}}$ is scattering wave vector and equals $k_0(\sin\theta_{\mathrm{s}}\hat{x} + \cos\theta_{\mathrm{s}}\hat{z})$. So the scattered wave can be written as

$$\varphi^{\mathrm{s}}_{\mathrm{KA}}(\vec{r}) = \sqrt{\frac{\mathrm{i}}{8\pi k_0 r}}\exp(\mathrm{i}kr)\varphi^{(N)}_{\mathrm{KA}}(\theta_{\mathrm{s}}), \tag{13}$$

where

$$\varphi^{(N)}_{\mathrm{KA}}(\theta_{\mathrm{s}}) = \int_s [(1+R)\varphi^{\mathrm{inc}}(\vec{r}')(-\mathrm{i}\vec{k}_{\mathrm{s}}\cdot\hat{n}') - (1-R)\frac{\partial\varphi^{\mathrm{inc}}(\vec{r}')}{\partial n'}]\exp(-\mathrm{i}\vec{k}_{\mathrm{s}}\cdot\vec{r}')\mathrm{d}s', \tag{14a}$$

$$\mathrm{d}s' = \sqrt{1+[f'(x')]^2}\,\mathrm{d}x'. \tag{14b}$$

The bistatic scattering coefficient $\sigma_1(\theta_{\mathrm{s}})$ in which the shadowing effect is neglected is defined as[13]

$$\frac{P_{\mathrm{s}}}{P_{\mathrm{inc}}} = \int_{-\pi/2}^{\pi/2}\sigma_1(\theta_{\mathrm{s}})\mathrm{d}\theta_{\mathrm{s}}, \tag{15}$$

where P_{inc} is the total power received by the rough surface and P_{s} is the scattered power by the rough surface. Finally, we have

$$\sigma_1(\theta_{\mathrm{s}}) = \frac{\left|\varphi^{(N)}_{\mathrm{KA}}(\theta_{\mathrm{s}})\right|^2}{\left[8\pi k_0 g\sqrt{\frac{\pi}{2}}\cos\theta_{\mathrm{i}}\left(1 - \frac{1+2\tan^2\theta_{\mathrm{i}}}{2k_0^2 g^2\cos^2\theta_{\mathrm{i}}}\right)\right]}. \tag{16}$$

The shadowing effect should be taken into account to rectify the bistatic scattering coefficient,

$$\sigma(\theta_{\mathrm{s}}) = S(\theta_{\mathrm{i}},\theta_{\mathrm{s}})\sigma_1(\theta_{\mathrm{s}}), \tag{17}$$

where $S(\theta_{\mathrm{i}},\theta_{\mathrm{s}})$ is the shadowing function, which can be expressed as

$$S(\theta_{\rm i},\theta_{\rm s})=\begin{cases}[1+\mathrm{erf}(v_{\rm s})]\,(1-\mathrm{e}^{-2B_{\rm s}})/(4B_{\rm s}) & 0^\circ\le\theta_{\rm s}\le\theta_{\rm i}\\ [1+\mathrm{erf}(v_{\rm i})]\,(1-\mathrm{e}^{-2B_{\rm i}})/(4B_{\rm i}) & \theta\le\theta_{\rm s}\le 90^\circ\\ [\mathrm{erf}(v_{\rm i})+\mathrm{erf}(v_{\rm s})]\,\{1-\exp[-2(B_{\rm i}+B_{\rm s})]\}/[4(B_{\rm i}+B_{\rm s})] & 90^\circ\le\theta_{\rm s}\le 180^\circ\end{cases}, \tag{18}$$

where $B_{\rm s/i}=\left\{\exp(-9v_{\rm s/i}^2/8)/(3\pi v_{\rm s/i}^2)^{1/2}+\exp(-v_{\rm s/i}^2)/(\pi v_{\rm s/i}^2)^{1/2}-[1-\mathrm{erf}(v_{\rm s/i})]\right\}/4$, $v_{\rm s/i}=\left|\tan\theta_{\rm s/i}\right|(l/\sqrt{2}h)$, $\mathrm{erf}(\cdot)$ is the error function. It should be noted that the two conditions of KA are also considered in our numerical simulations.

Let $\varphi(\vec{r})$ and $\varphi_1(\vec{r})$ denote the total wave function for the upper medium and the lower medium, respectively, and they satisfy the following integral equations[9]:

$$\frac{1}{2}\varphi(\vec{r})-\int_s\left[\varphi(\vec{r}\,')\frac{\partial G(\vec{r},\vec{r}\,')}{\partial n'}-G(\vec{r},\vec{r}\,')\frac{\partial\varphi(\vec{r}\,')}{\partial n'}\right]\mathrm{d}s'=\varphi^{\rm inc}(\vec{r}), \tag{19a}$$

$$\frac{1}{2}\varphi_1(\vec{r})+\int_s\left[\varphi_1(\vec{r}\,')\frac{\partial G_1(\vec{r},\vec{r}\,')}{\partial n'}-G_1(\vec{r},\vec{r}\,')\frac{\partial\varphi_1(\vec{r}\,')}{\partial n'}\right]\mathrm{d}s'=0, \tag{19b}$$

where $G_1(\vec{r},\vec{r}\,')=\frac{1}{4}H_0^{(1)}(k_1\left|\vec{r}-\vec{r}\,'\right|)$ is the Green function of the lower medium, k_1 is the wave number of the lower medium. Using MOM to discretize the two integral equations, the matrix equation of the problem is[9]

$$\begin{bmatrix}A & B\\ \rho A^{(1)} & B^{(1)}\end{bmatrix}\begin{bmatrix}u(x)\\ \nu(x)\end{bmatrix}=\begin{bmatrix}\varphi^{\rm inc}\\ 0\end{bmatrix}, \tag{20}$$

where A, B, $A^{(1)}$, $B^{(1)}$ are four block matrices and $u(x)/\sqrt{1+[f'(x)]^2}$, $v(x)$ are unknowns, which correspond to the surface electric field and magnetic field, respectively. For HH polarization, $\rho=1$ and for VV polarization, $\rho=\varepsilon_1$. The elements of the matrices are not present here due to the space limitation. Solving the matrix equation by the conjugate gradient method (CGM)[9], the scattered wave function is obtained as

$$\varphi^{\rm s}_{\rm MOM}(\vec{r})=\sqrt{(\mathrm{i}/8\pi k_0 r)}\exp(\mathrm{i}k_0 r)\varphi^{(N)}_{\rm MOM}(\theta_{\rm s}), \tag{21}$$

where

$$\begin{aligned}&\varphi^{(N)}_{\rm MOM}(\theta_{\rm s})\\ &=-\int_s\mathrm{d}x'\{-u(x')+\nu(x')\mathrm{i}k_0[f'(x')\sin\theta_{\rm s}-\cos\theta_{\rm s}]\}\\ &\quad\times\exp(-\mathrm{i}\vec{k}_{\rm s}\cdot\vec{r}\,').\end{aligned} \tag{22}$$

The definition of the bistatic scattering coefficient is the same as that by Eq. (15). The bistatic scattering coefficient calculated by MOM finally can be written as

$$\sigma(\theta_{\rm s})=\frac{\left|\varphi^{(N)}_{\rm MOM}(\theta_{\rm s})\right|^2}{\left[8\pi k_0 g\sqrt{\frac{\pi}{2}}\cos\theta_{\rm i}\left(1-\frac{1+2\tan^2\theta_{\rm i}}{2k_0^2g^2\cos^2\theta_{\rm i}}\right)\right]}. \tag{23}$$

Hence, the definitions of the bistatic scattering coefficients of 1D rough surface scattering calculated by KA and MOM are unified, just as those given in Eqs. (16) and (23), respectively.

In the following numerical implementations, the wavelength of the incident wave is 0.6328 μm and the incident angle is 30° for HH polarization. In order to examine the validity of the modified KA, the bistatic scattering coefficient calculated by MOM with Eq. (23) and the modified KA with Eq. (16) are firstly compared in Figs. 2(a) and (b) for HH and VV polarization, respectively. From Fig. 2, it can be concluded that by introducing the tapered wave into the classical KA and the redefinition of the scattering coefficient calculated by KA, the bistatic scattering coefficient calculated by both MOM and the modified KA are almost identical for the whole scattering regions.

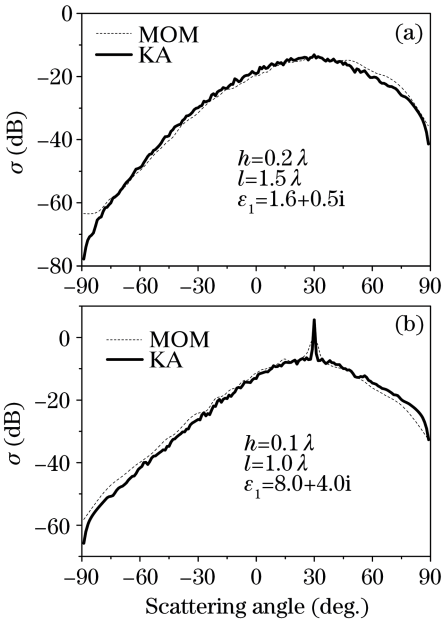

Fig. 2. Comparison of scattering coefficients calculated by MOM and KA for (a) HH polarization and (b) VV polarization.

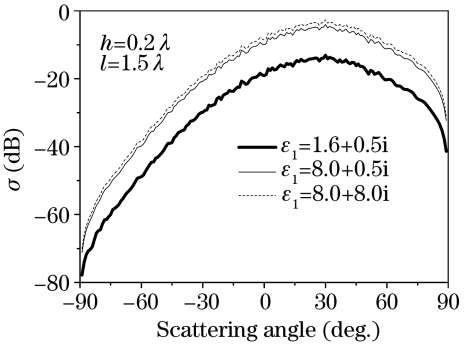

Fig. 3. Scattering distribution of σ for different ε_1.

To further explore the dependences of the optical wave scattering on the parameters of Gaussian random rough surface, the scattering distribution of σ for different values of ε_1, h, and l are calculated by MOM, and the results are shown in Figs. $3-5$. In Fig. 3, the influence of ε_1 on σ is plotted. It is observed that as the real part of ε_1 increasing, the scattering coefficient increases more rapidly than that of the imaginary part, in other words, the scattering coefficient is not sensitive to the variation of the imaginary part. Figure 4 depicts the scattering pattern of σ for different h. It is shown that with the increase of h, the scattering coefficient near the specular direction (mainly corresponding to the coherent component) decreases, whereas the incoherent component in the non-specular direction increases. Another point worth noting is that for $h = 0.1\lambda$, the scattering coefficient in the specular direction has a more obvious peak than the result of $h = 0.4\lambda$, this phenomenon mainly results from the fact that the roughness of the Gaussian surface increases with larger h. Further illustration of the effect of the correlation length l on the angular of σ is presented in Fig. 5. It is found that the influence of l on the scattering coefficient σ is significant, especially for the non-specular direction. The primary reason is that for the smaller l, the height of Gaussian rough surface varies more heavily, which leads to a more incoherent scattering contribution to the bistatic scattering coefficient in the non-specular direction. As apparently shown in Fig. 5, the larger l is, the larger the scattering coefficient will be for the same scattering angle away from the specular direction.

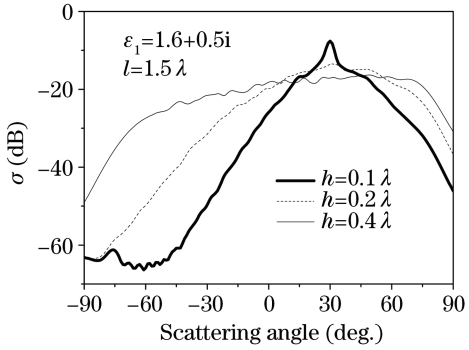

Fig. 4. Scattering distribution of σ for different h.

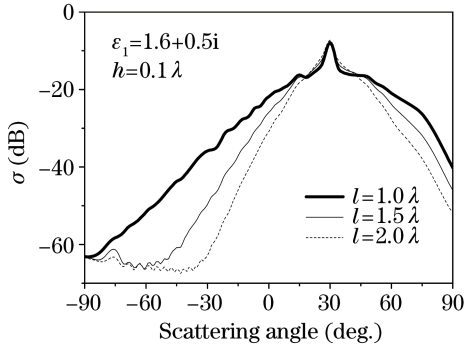

Fig. 5. Scattering distribution of σ for different l.

In conclusion, by introducing the tapered incident wave, taking into account the shadowing effect, and redefining the classical KA for calculating optical wave scattering from 1D lossy dielectric Gaussian rough surfaces, the scattering coefficient calculated by KA agrees very well with that by MOM. The characteristics of the optical wave scattering from the lossy dielectric Gaussian random rough surface for different parameters, such as the lossy dielectric constant, the correlation length, and the RMS height, are analyzed by implementing MOM. The optical scattering pattern by the lossy dielectric Gaussian random rough surface is found to be heavily influenced by these parameters.

This work was supported by the National Natural Science Foundation of China (No. 60571058) and the Specialized Research Fund for the Doctoral Program of Higher Education, China (No. 20070701010).

References

1. J. Krč, F. Smole, and M. Topič, Prog. Photovolt. Res. Appl. **11,** 15 (2003).
2. D. Didascalou, M. Döttling, N. Geng, and W. Wiesbeck, IEEE Trans. Antenn. Propag. **51,** 1508 (2003).
3. A. E. Babayan, N. L. Margaryan, and Kh. V. Nerkararyan, Photon. Nanostruct. **4,** 35 (2006).
4. D. Xiang and W.-H. Huang, Nucl. Instrum. Methods Phys. Res. B **248,** 163 (2006).
5. L. Guo, Y. Wang, and Z. Wu, Chin. Opt. Lett. **2,** 431 (2004).
6. X. Ren and L. Guo, Chin. Opt. Lett. **5,** 605 (2007).
7. M. E. Knotts, T. R. Michel, and K. A. O'Donnell, J. Opt. Soc. Am. A **9,** 1822 (1992).
8. E. I. Thorsos, J. Acoust. Soc. Am. **83,** 78 (1988).
9. L. Tsang, J. A. Kong, K.-H. Ding, and C. O. Ao, *Scattering of Electromagnetic Waves: Numerical Simulations* (Wiley, New York, 2001) p.115.
10. J. A. Ogilvy, *Theory of Wave Scattering from Random Rough Surfaces* (IOP Publishing, Bristol, 1991) p.73.
11. X. Wang, Y.-B. Gan, and L.-W. Li, IEEE Antenn. Wireless Propag. Lett. **2,** 319 (2003).
12. H. Ye and Y.-Q. Jin, IEEE Trans. Antenn. Propag. **53,** 1234 (2005).
13. Q. Li, C. H. Chan, and L. Tsang, IEEE Trans. Antenn. Propag. **47,** 752 (1999).